Trees
DOI 10.1007/s00468-017-1552-4

ORIGINAL ARTICLE

Immunolocalization of pectin and hemicellulose epitopes in the phloem of Norway spruce and Scots pine

Jong Sik Kim[1] · **Geoffrey Daniel**[1]

Received: 14 November 2016 / Accepted: 12 April 2017

Abstract
Key message **Distribution patterns of pectin and hemicellulose epitopes in the phloem of Pinaceae conifers differ between cell types including sieve cells, axial/ray parenchyma cells and stone cells, which is more prominent in seedlings than mature trees.**
Abstract Although there is considerable information on the gross chemistry of conifer bark, little is known on the chemistry of secondary phloem at the individual cell level. This study investigated distribution of pectins and hemicelluloses in the phloem of two conifer species (Norway spruce and Scots pine) at an individual cell wall level using nine monoclonal antibodies specific for pectin and hemicellulose epitopes combined with immunofluorescence and TEM immunogold labeling. Differences in phloem cell wall chemistry between juvenile (seedlings) and mature conifer trees were also examined. The two conifer species showed qualitatively similar distribution patterns of epitopes in sieve- and (axial/ray) parenchyma cells, irrespective of seedlings and mature trees. Sieve- and parenchyma cell walls showed the presence of rhamnogalacturonan-I (RG-I), homogalacturonan (HG) and xyloglucan epitopes, but revealed the absence of heteroxylan epitopes. Heteromannan epitopes were only detected in sieve cell walls, showing a chemical difference between sieve- and parenchyma cells. In contrast to qualitative similarity, there were several quantitative differences of epitope localization in sieve- and parenchyma cells between the two conifer species, indicating variations in the chemical structure and/or the amount of pectins and hemicelluloses between the two conifer species. These differences were more significant in seedlings than mature trees. Immunogold labeling of Norway spruce seedlings further indicated the possibility of chemical variations between cell wall regions within a single sieve cell wall. Phloem stone cells detected in mature Norway spruce showed the presence of heteromannans/heteroxylans and RG-I/HG/xyloglucans in secondary cell wall and middle lamellae, respectively.

Keywords Hemicellulose · Parenchyma cell · Pectin · Sieve cell · Softwood · Stone cell

Introduction

In a tree stem, the phloem (secondary) represents the inner layer of bark whose anatomical structure differs significantly from xylem (secondary) even though the two tissues are originated from the same vascular cambium. While xylem is responsible for transporting water and solutes, phloem primarily regulates the long-distance transport of photoassimilates and signals throughout the tree stem (Jyske and Hölttä 2015). Phloem also plays an important role in mechanical and chemical defense against beetles and pathogens, particularly in conifers (Franceschi et al. 2005; Whitehill et al. 2015). As part of the bark, phloem is also been important traditionally for production of industrially important secondary metabolites and is currently

Communicated by J. Lin.

Electronic supplementary material The online version of this article (doi:10.1007/s00468-017-1552-4) contains supplementary material, which is available to authorized users.

✉ Geoffrey Daniel
geoffrey.daniel@slu.se

[1] Wood Science, Department of Forest Products, Swedish University of Agricultural Sciences, P.O. Box 7008, 750 07 Uppsala, Sweden

Published online: 22 April 2017

viewed as a potential resource for biorefineries (e.g., Le Normand et al. 2014).

With respect to conifers, phloem is composed mainly of sieve cells, albuminous cells, axial/ray parenchyma cells and sclerenchyma cells. Sieve cells are the main cell type contributing to long-distance transportation and are functionally supported by albuminous cells (Evert 1977). Unlike other gymnospermous sieve cells (i.e., have primary cell walls), sieve cells of the Pinaceae including Norway spruce and Scots pine examined in this study have thickened cell walls, which are considered as representing secondary cell walls (Abbe and Crafts 1939; Evert 1977). Axial/ray parenchyma cells are living cells and major sites for storage of starch and/or lipids. Axial parenchyma cells normally contain phenolic compounds and are called polyphenolic parenchyma (PP) cells (Franceschi et al. 2005). Sclerenchyma cells have thick secondary cell walls and the amount and morphological form vary greatly between conifer species (Franceschi et al. 2005; Whitehill et al. 2015). Considering phloem chemistry, although there is considerable information on gross chemistry of conifer bark (Harun and Labosky 1985; Kemppainen et al. 2012; Kofujita et al. 1999; Nurmi 1997; Rhén 2004; Umemura et al. 2014), little is known on the chemistry of actual secondary phloem (Jyske et al. 2015; Li et al. 2007). Also there is limited information available on the chemistry of conifer phloem at the individual cell level since separation of individual cell types from phloem tissue for chemical analysis is not on easy task. In particular, little information is available on the distribution of pectins and hemicelluloses in conifer phloem at the individual cell level including stone cells (Whitehill et al. 2015) and epithelial cells in resin ducts (Kim and Daniel 2014). The role of these polysaccharides in various biological processes associated with phloem cell development (e.g., lignification) and defense response is also poorly understood in conifer.

Glycan-directed probes such as monoclonal antibodies coupled with immunolocalization techniques are important tools to gain temporal and spatial information on the distribution of plant cell wall components and their diversity between cell types, information which cannot be provided using classical wet chemical analysis (Knox 2008). This type of cellular information is essential for a better understanding of the molecular basis of cell wall function and development (Knox 2008). In this study, we examined the chemical features of conifer phloem at an individual cell wall level using nine monoclonal antibodies specific for pectin and hemicellulose epitopes combined with immunofluorescence and immunogold labeling. Differences in phloem cell wall chemistry between juvenile (seedlings) and mature conifer trees were also explored in the study.

Materials and methods

Plant materials

Two year old Norway spruce (*Picea abies* L. Karst) and Scots pine (*Pinus sylvestris* L.) seedlings from a commercial nursery (Lugnets Plantskola, Sweden) and mature Norway spruce and Scots pine grown at a forest site near the campus of the Swedish University of Agricultural Sciences were used for the study. Several small sectors (5–10) containing phloem, cambium and xylem were taken from stems of seedlings [ca. 7/9 mm (spruce/pine) in diameter at 2–3 cm above ground level] and mature trees [ca. 25.4/24.8 cm (spruce/pine) in diameter at 1.3 m above ground level] on August 8 and September 16, respectively. Sectors were fixed in a mixture of 2.5% v/v glutaraldehyde and 2% v/v paraformaldehyde in 0.05 M sodium cacodylate buffer (pH 7.2) for 4 h at room temperature. After dehydration through a graded ethanol series, sectors were embedded in LR White resin (London Resin Co., Basingstoke, UK) according to procedures described previously (Kim and Daniel 2012a, b). Fresh samples were used without embedding for phloroglucinol-HCl staining (Wiesner reaction, Kim and Daniel 2014).

Light and fluorescence microscopy

Immunofluorescence labeling was conducted according to procedures described previously (Kim and Daniel 2012a, b). In brief, semi-thin sections (ca. 1 µm) from embedded wood blocks mounted on glass slides coated with silane (Sigma, St. Louis, USA) were incubated with either LM5 (galactan), LM6 (arabinan), LM10/LM11 (heteroxylan), LM15 (xyloglucan), LM19/LM20 (homogalacturonan, HG) or LM21/LM22 (heteromannan) monoclonal antibodies (PlantProbes, Leeds, UK), followed by incubation with anti-rat IgG Alexa Fluor 488 (Invitrogen, Oregon, USA). For controls, sections were incubated with Alexa Fluor 488 only. Sections were examined using fluorescence microscopy (Leica DMRE, Wetzlar, Germany) and I3 filter cube (excitation 450–490 nm, emission >515 nm). Fluorescence images were captured using Leica DFC 490 digital camera (Heerbrugg, Switzerland). For observations of general anatomy, some serial sections were examined using light microscopy (Leica DMLB, Wetzlar, Germany) after staining with 1% w/v toluidine blue in 0.1% borax buffer.

To examine the masking effects of pectic HG on detection of hemicellulose epitopes, semi-thin sections mounted on glass slides were pre-treated with 0.1 M sodium carbonate (pH 11.4) for 2 h at room temperature, followed by 30 U/ml pectate lyase (from *Aspergillus* sp.,

Megazyme, Wicklow, Irland) in 50 mM CAPS (3-(cyclohexylamino)-1-propanesulfonic acid) buffer (pH 10.0) containing 2 mM $CaCl_2$ for 2 h at room temperature (Lee and Knox 2014). After several washes with distilled water, immunofluorescence labeling was conducted and examined as described above. As control, equivalent sections were also pre-treated only with sodium carbonate prior to labeling. Removal of pectins was examined using the LM19 antibody. Sections, which were omitted from pectate lyase treatment served as controls. Results of immunofluorescence labeling including the enzymatic pre-treatment reflect observations on two different serial sections of each tree sample, which were randomly selected from embedded blocks.

Transmission electron microscopy (TEM)

To examine the possibility of heterogeneity in the microdistribution of epitopes within a single sieve cell wall, immunogold labeling was also carried out on Norway spruce seedlings according to the procedures described previously (Kim and Daniel 2012a, b). In brief, ultrathin sections (ca. 90 nm) mounted on nickel grids were incubated with the monoclonal antibodies described above, followed by incubation with secondary antibody labeled with 10-nm colloidal gold particles (BB International, Cardiff, UK). Sections were examined using a Philips CM12 TEM (Philips, Eindhoven, The Netherlands) after staining with uranyl acetate. No non-specific binding of secondary antibody (gold particles) was detected in control samples where the primary antibody was omitted (not shown). Results reflect observations on two different sections.

Results

Phloem anatomy, cell classification and lignification

Phloem anatomy of the tree samples studied is shown in Fig. 1 and Supplementary Figure 1. In xylem, no notable formation of compression wood was detected in all tree samples (not shown). Mature Norway spruce and Scots pine showed almost the end of cambial growth. Norway spruce and Scots pine seedlings revealed active cambial growth, showing formation of latewood and transition wood in xylem, respectively. Mature trees showed a clear growth ring of phloem (Supplementary Fig. 1b, c), which was determined by an annual tangential ring of polyphenolic parenchyma cells (Franceschi et al. 2005). In contrast, growth rings of phloem were unclear in the two seedlings (Fig. 1a, Supplementary Fig. 1a). Chemical characteristics of non-collapsed phloem cells (i.e., current growth ring) are mainly described in the study with a focus on sieve cells and (axial/ray) parenchyma cells. Classification of albuminous cells was avoided in this study since the anatomical distinction between albuminous cells and other phloem parenchyma cells (axial) was difficult. Sieve cells with thickened walls were considered as the mature or final stage of differentiation. Thin-walled cells (asterisks in Fig. 1b, c) and convex cells (marked 5 in Fig. 1a, asterisks in Fig. 4e and Supplementary Fig. 1c) were unspecified in this study. These cells showed differences in distribution patterns of epitopes from thickened sieve cells in the study (see below). Unlike mature trees, the two seedlings showed notable differences in distribution of epitopes between the two anatomical regions within the phloem studied. For comparison, phloem of the two seedlings was classified as late phloem which was developed recently (marked 1–8 in Fig. 1a and inset, 1–6 in Fig. 1c) and early phloem that was developed earlier. Axial parenchyma cells frequently contained phenolic compounds (Fig. 1). Stone cells were only detected in collapsed phloem of mature Norway spruce in this study (Fig. 10). A positive Wiesner reaction (phloroglucinol-HCl staining) for lignin was only detected in stone cells of mature Norway spruce (Supplementary Fig. 2).

Detection of pectin epitopes in sieve- and parenchyma cells

No non-specific binding of secondary antibodies (i.e., Alexa 488) was detected in control samples, where the primary antibodies were omitted. Immunofluorescence images described below were captured based on the control image shown in Fig. 2b, which showed lack of any significant contribution of autofluorescence except for phenolic compounds located in axial parenchyma cell lumina.

Distribution of rhamnogalacturonans-I (RG-I) was examined using LM5 and LM6 antibodies (Knox 2008) that bind to epitopes of (1 → 4)-β-galactans (Jones et al. 1997) and (1 → 5)-α-arabinans (Willats et al. 1998), respectively. There is also a possibility of the binding of the LM6 antibody to arabinogalactan-proteins (AGPs) (Lee et al. 2005) even though it was not considered in the study. LM5 bound mainly to parenchyma cell walls in the two tree species, no matter tree age (Fig. 2). Only weak and partial binding of LM5 was detected in sieve cell walls except for pine seedling that showed some strong labeling in sieve cells of late phloem (marked 1–6 in Fig. 2c). With immunogold labeling in spruce seedling, LM5 epitopes were only detected in the cell corner middle lamellae of a few sieve cells (inset in Fig. 2a).

LM6 bound to all sieve- and parenchyma cells of all tree samples. However, there were some differences in distribution patterns of epitopes between species and between

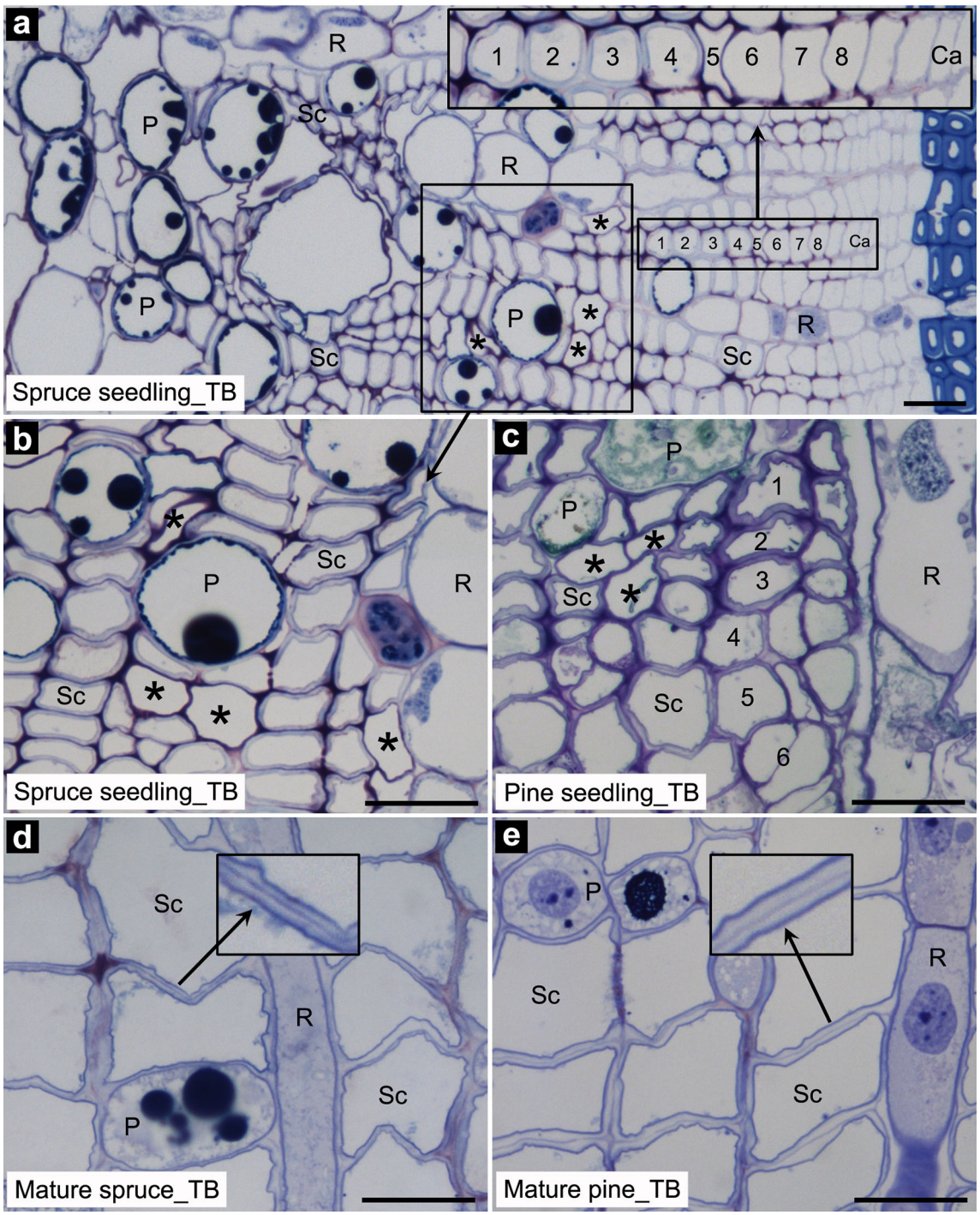

Fig. 1 Anatomy of Norway spruce and Scots pine phloem. **a**, **b** Phloem of Norway spruce seedling stained with toluidine blue (TB). Numbers *1–8* are classified as late phloem in the study. Note thickened sieve cell walls (Sc; marked *1–4* in *inset* of **a**, **b**), unspecified thin-walled cells (*asterisks* in **a**, **b**), convex cells (marked *5* in **a**) and polyphenolics in axial parenchyma cells (P). **c** Phloem of Scots pine seedling stained with TB. Numbers *1–6* are classified as late phloem in the study. Note the presence of unspecified thin-walled cells (*asterisks*) together with thickened sieve cells. **d**, **e** Phloem of mature Norway spruce and Scots pine stained with TB. Note thickened sieve cell wall with stronger staining in the innermost layer of sieve cells (*insets*). Each number in **a**, and **c** (i.e., seedlings) indicates the same cell in immunofluorescence images (Figs. 2, 3, 4, 5, 6, 7). *Ca* cambium, *R* ray parenchyma cell. *Scale bars* 25 µm

tree ages. In seedlings, spruce showed more abundant LM6 epitopes in parenchyma- than sieve cells (Fig. 3a), whereas pine showed slightly less abundant epitopes in parenchyma- than sieve cells (Fig. 3c). Overall, LM6 epitopes in sieve cells were also more abundant in pine- than spruce seedling (Fig. 3a, c). Sieve cells of late phloem

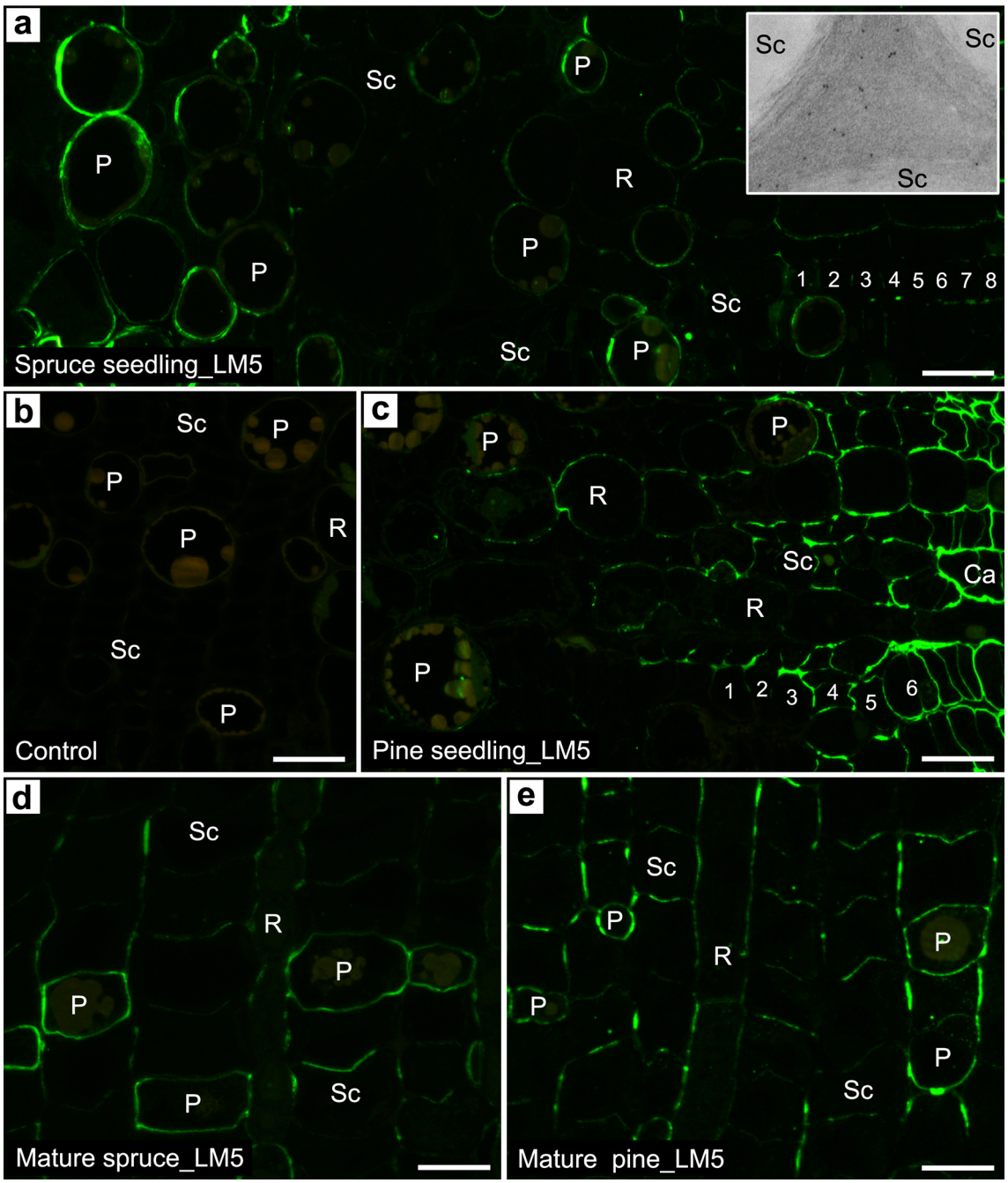

Fig. 2 Detection of (1 → 4)-*β*-galactan (LM5) epitopes in phloem cells. **a** Norway spruce seedling showing very sparse epitopes in sieve cells (Sc); only in cell corner middle lamellae of a few sieve cells (*inset*). Note presence of epitopes in (axial/ray) parenchyma cells (P/R) with a variation in the amount of epitopes between cells. **b** Control with primary antibody omitted. Note strong autofluorescence of polyphenolics in parenchyma cells. **c** Scots pine seedling showing some strong labeling in sieve cells of late phloem (marked *1–6*) and sparse epitopes in (axial/ray) parenchyma cells (P/R). **d**, **e** Mature Norway spruce and Scots pine, respectively, showing sparse epitopes with more abundance in parenchyma- than sieve cells. Note some partial/or random distribution of epitopes in sieve cell walls. *Scale bars* 25 µm

(marked 1–4 in Fig. 3a and 1–6 in Fig. 3c) revealed more abundant LM6 epitopes compared to those of early phloem in both seedlings. Compared to seedlings, differences in distribution of LM6 epitopes were less prominent in mature trees (Fig. 3d, e). LM6 epitopes in sieve cells were similar or slightly more abundant than those in parenchyma cells in

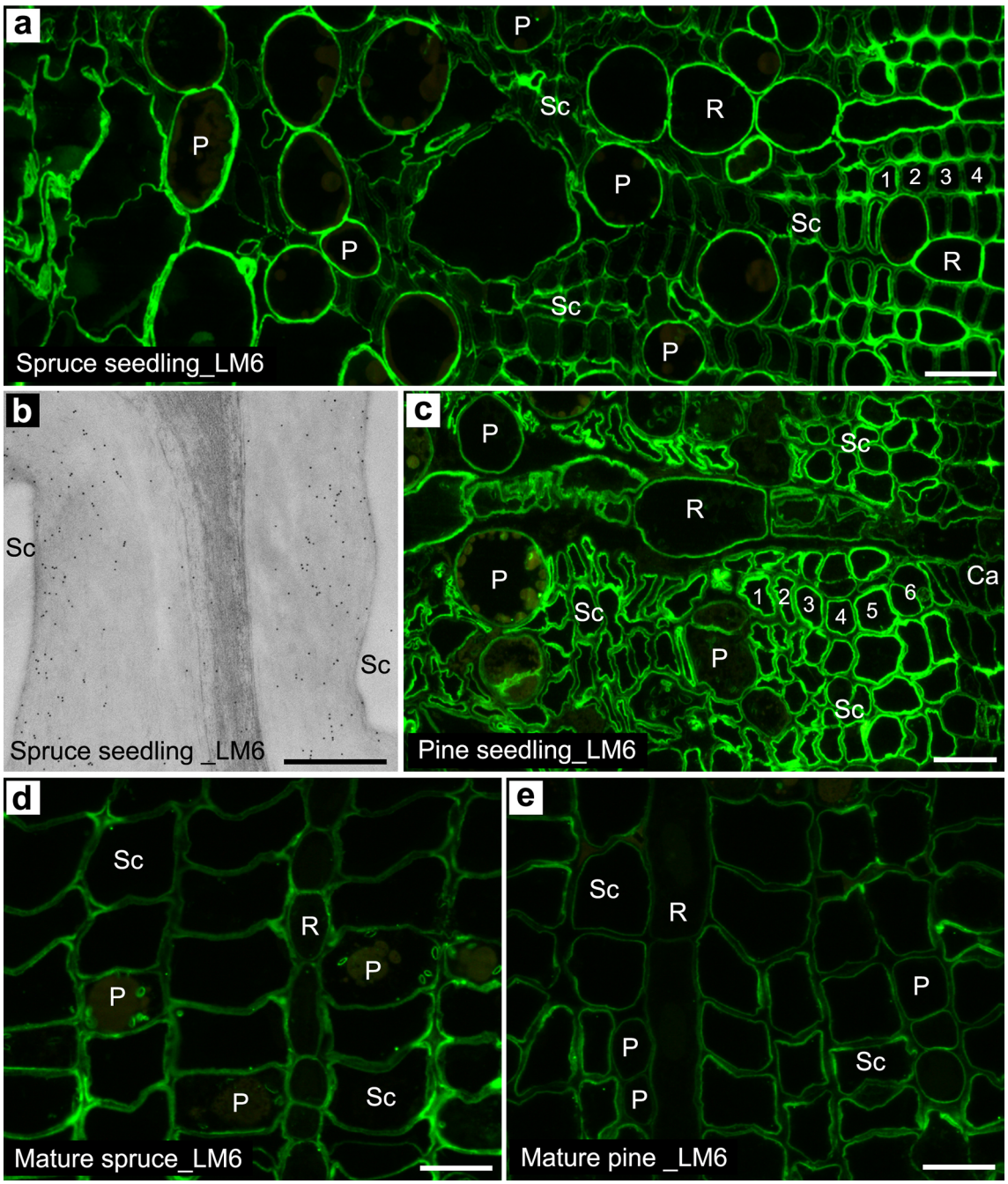

Fig. 3 Detection of (1 → 5)-α-arabinan (LM6) epitopes in phloem cells. **a** Norway spruce seedling showing overall more abundant epitopes in (axial/ray) parenchyma cells (P/R) than sieve cells (Sc). Note more abundant epitopes in sieve cells of late phloem (marked *1–4*) than those in early phloem. **b** Immunogold labeling of Norway spruce seedling showing more abundant epitopes in the inner- than outer sieve cell wall with very sparse epitopes in middle lamellae. **c** Scots pine seedling showing overall more abundant epitopes in sieve cells compared to spruce seedling (**a**) in both early- and late (marked *1–6*) phloem. Note slightly more abundant epitopes in sieve- than parenchyma cells (i.e., opposite to spruce seedling) and the absence of epitopes in middle lamellae of sieve cells. **d**, **e** Mature Norway spruce and Scots pine, respectively, showing slightly more abundant epitopes in sieve- than parenchyma cells. Note absence of epitopes in middle lamellae of sieve cells. *Ca* cambium. *Scale bars* 25 µm (**a**, **c**–**e**), 500 nm (**b**)

both mature trees (Fig. 3d, e). Sieve cells in spruce seedling showed more abundant LM6 epitopes in the inner- than outer cell walls with sparse epitopes in middle lamella regions (Fig. 3b).

Distribution of homogalacturonans (HG) was studied using LM19 (binds to partial methyl-esterified- and un-esterified HG, low methyl-esterified HG) and LM20 (binds only to methyl-esterified HG, high methyl-esterified HG)

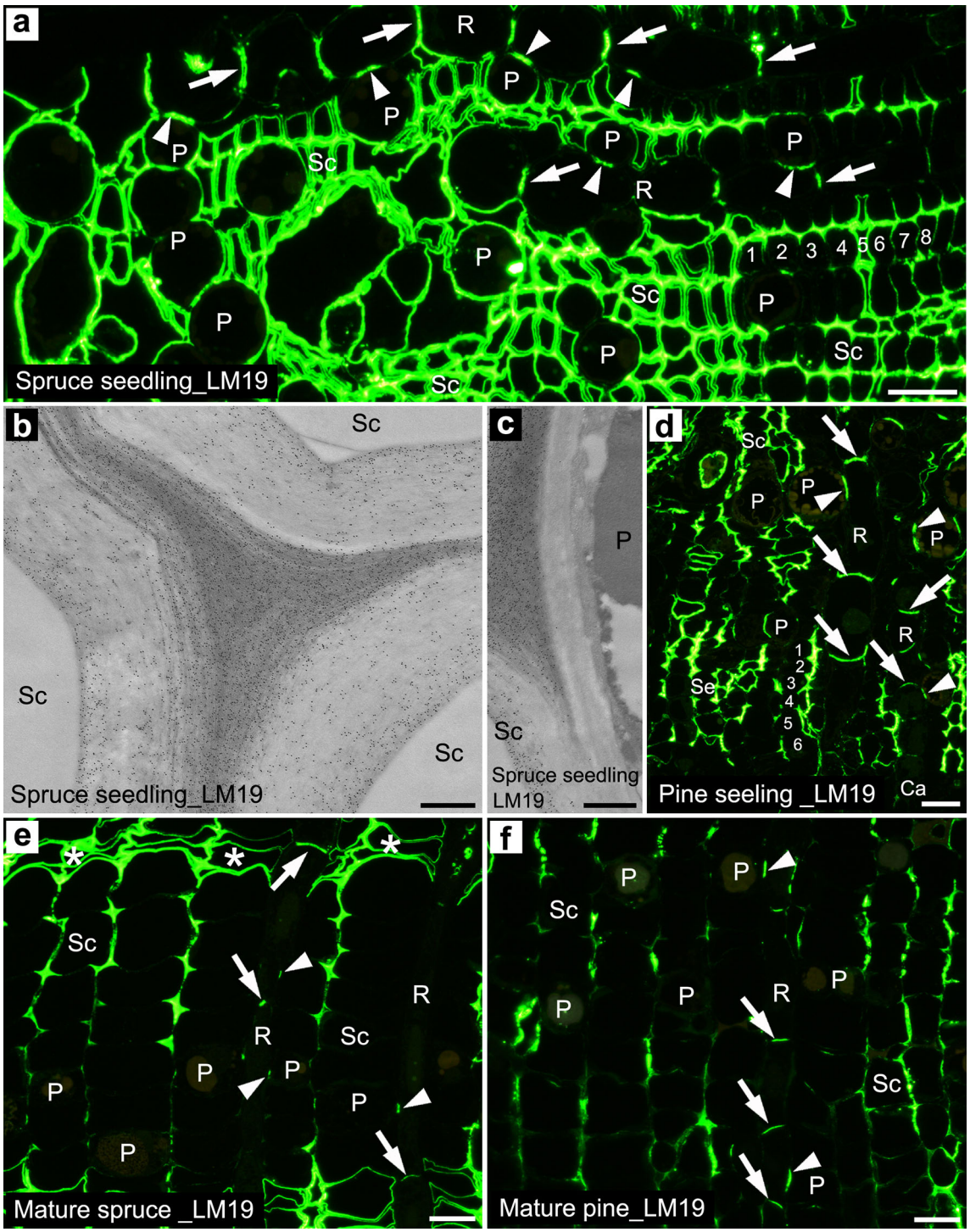

Fig. 4 Detection of un/low methyl-esterified homogalacturonan (HG, LM19) epitopes in phloem cells. **a** Norway spruce seedling showing abundant epitopes in sieve cells (Sc) of early phloem. Epitopes in thickened sieve cells of late phloem (marked *1–4*) were mostly restricted to radial cell walls. **b**, **c** Immunogold labeling of Norway spruce seedling showing abundant epitopes in sieve cell walls of early phloem including middle lamellae with more abundance in the inner (lumen side)- than outer cell (**b**). Note the absence of epitopes in axial parenchyma cell wall (**c**). (**d**) Scots pine seedling showing much lesser amounts of epitopes in sieve cells compared to spruce seedling (**a**). Overall epitopes were more abundant in radial- than tangential sieve cells with a high variation in the amount between cells. **e**, **f** Mature Norway spruce and Scots pine respectively showing restricted localization of epitopes in radial sieve cell walls. Note restricted localization of epitopes to axial parenchyma cell walls (P) in contact with ray parenchyma cells (*arrowheads* in **a**, **d**–**f**) and tangential cell wall of ray parenchyma cells (*arrows* in **a**, **d**–**f**) in all tree samples. Note also abundant epitopes in convex cells of Norway spruce (marked *5* in **a**; *asterisks* in **e**). *Ca*, cambium. *Scale bars* 25 µm (**a**, **d**–**f**), 500 nm (**b**, **c**)

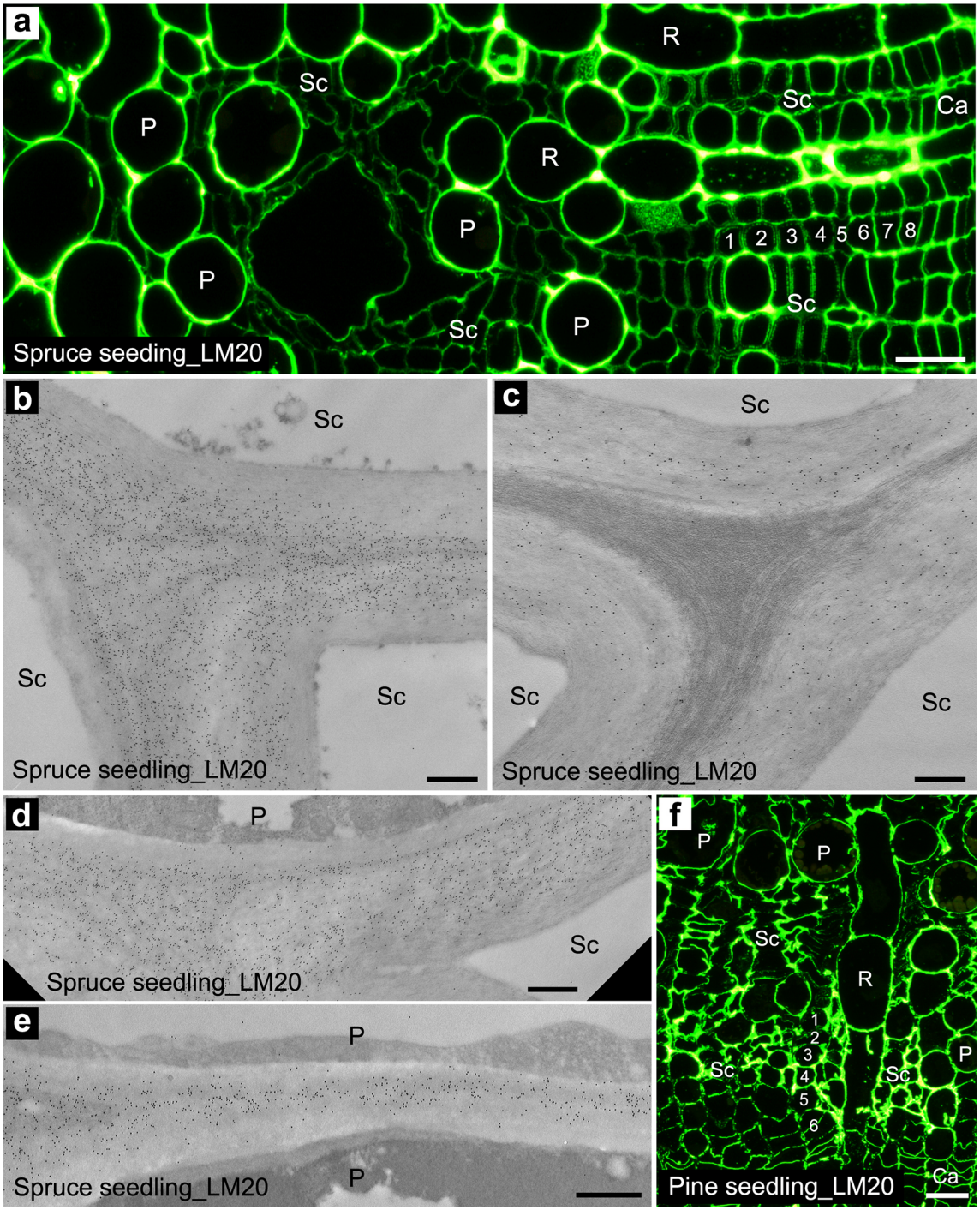

Fig. 5 Detection of highly methyl-esterified homogalacturonan (HG, LM20) epitopes in phloem cells. **a** Norway spruce seedling showing more abundant epitopes in (axial/ray) parenchyma (P/R)- than sieve cells (i.e., opposite to LM19 epitopes, Fig. 4a). **b–e** Immunogold labeling of Norway spruce seedling showing much more abundant epitopes in sieve cells of late phloem (**b**) compared to those of early phloem (**c**). Note much more abundant epitopes in sieve cell walls joined to parenchyma cells (**d**) than those further away from parenchyma cells (**c**) in early phloem. Epitopes in sieve cells (**b–d**) and axial parenchyma cells (**e**) are detected mostly in the outer (middle lamella side) cell wall layers. **f** Scots pine seedling showing overall more abundant epitopes in sieve cells of early phloem compared to spruce seedling (**a**) with a high variation in the amount of epitopes between sieve cells. Note more uniform distribution of epitopes between ray- and tangential sieve cell wall in late (marked *1–6*)- than early phloem. *Ca* cambium. *Scale bars* 25 µm (**a**, **f**), 500 nm (**b–e**)

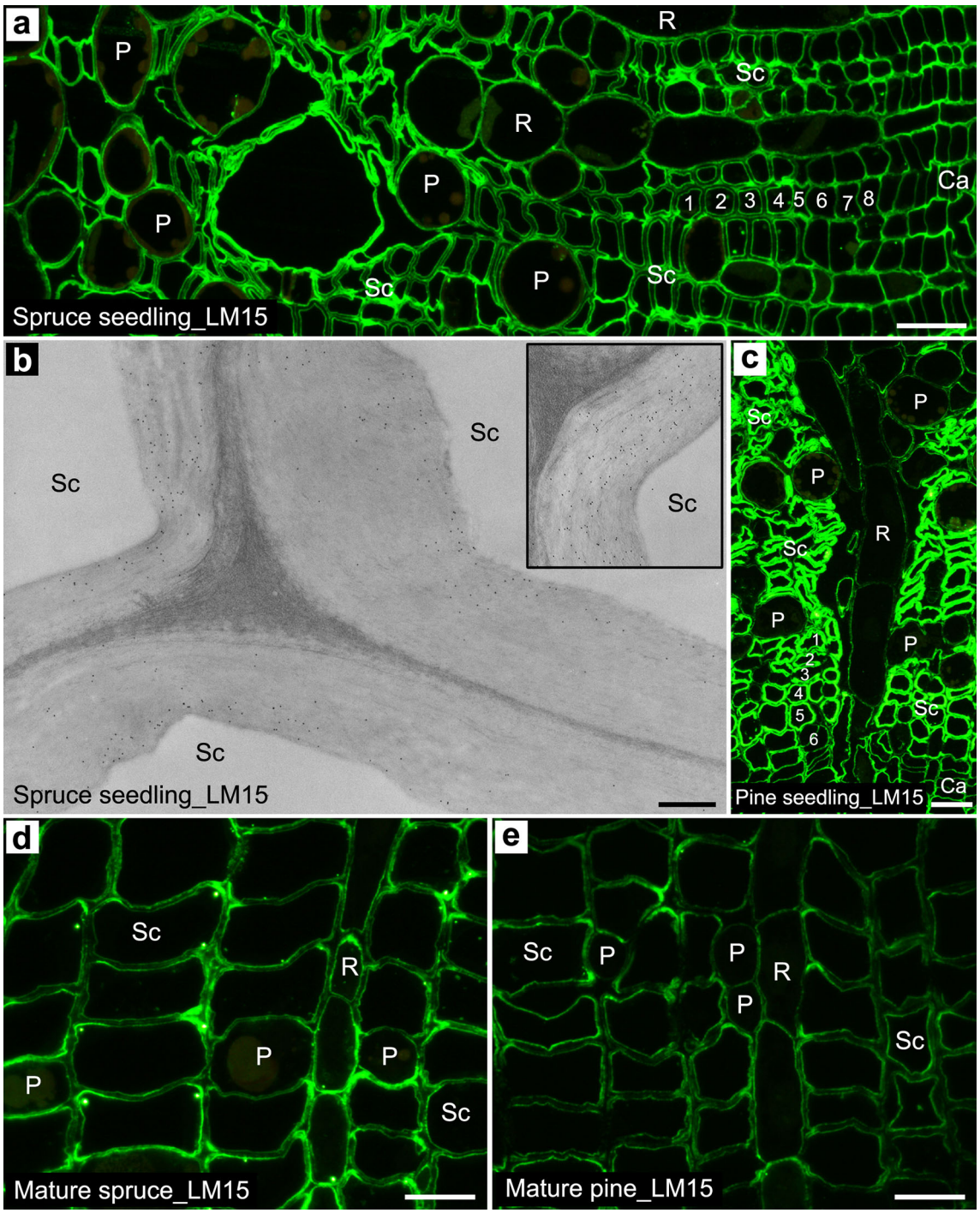

Fig. 6 Detection of xyloglucan (LM15) epitopes in phloem cells. **a** Norway spruce seedling showing the presence of epitopes in sieve cells (Sc) and (axial/ray) parenchyma cells (P/R) with similar intensity of labeling. **b** Immunogold labeling of Norway spruce seedling showing that epitopes in thickened sieve cell were mostly localized in the inner cell wall layer except for a few sieve cells that showed uniform distribution across the cell wall (*inset*). Note the absence of epitopes in middle lamellae of sieve cells. **c** Scots pine seedling showing more uniform and abundant epitopes in sieve cells compared to spruce seedling (**a**). Note much more abundant epitopes in sieve- than parenchyma cells (i.e., differ from spruce seedling). **d**, **e** Mature Norway spruce and Scots pine, respectively, showing similar distribution patterns of epitopes to spruce seedling (**a**). Note almost absence of epitopes in middle lamellae of sieve cells. *Ca* cambium. *Scale bars* 25 µm (**a**, **c**–**e**), 500 nm (**b**)

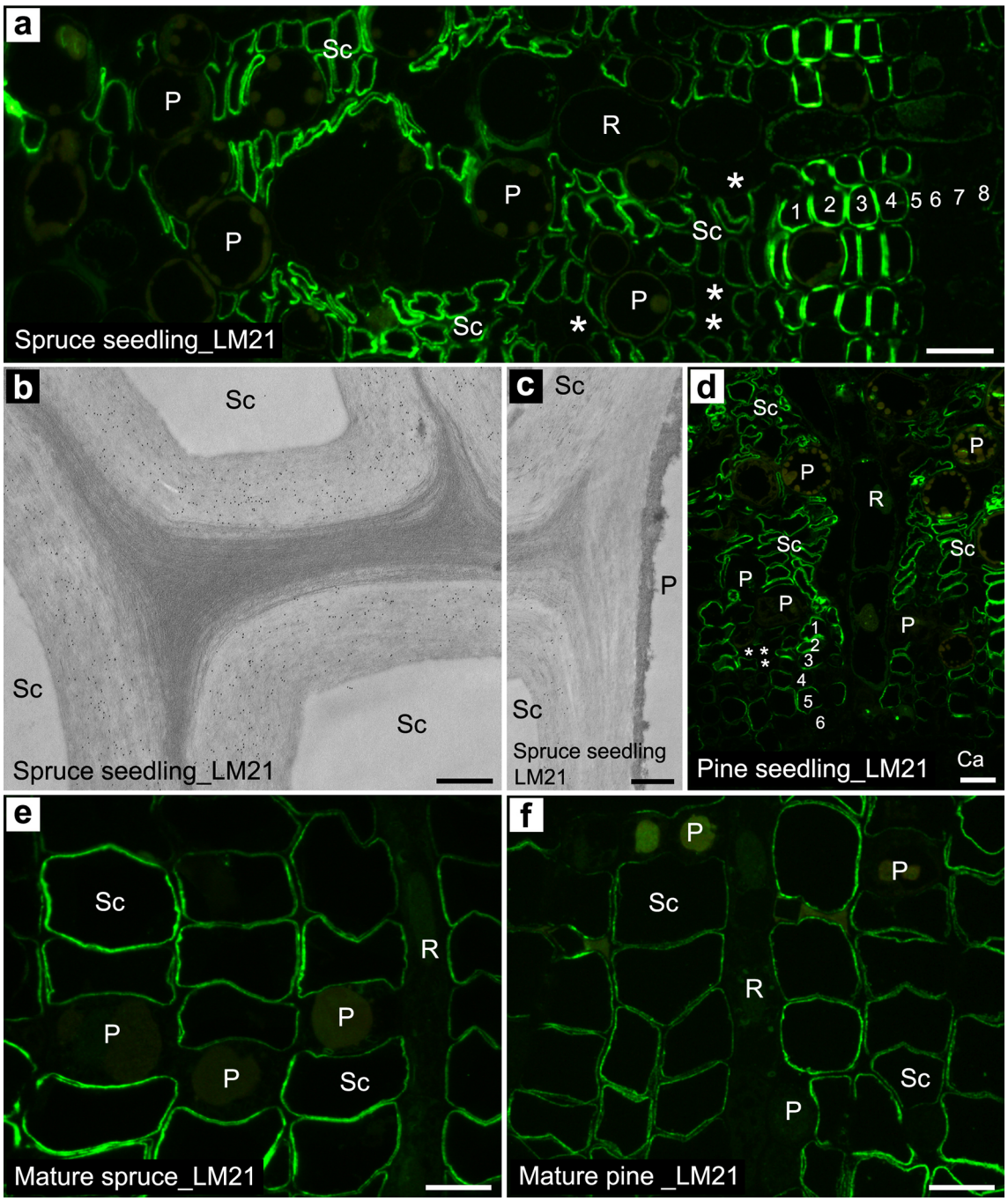

Fig. 7 Detection of heteromannan (LM21) epitopes in phloem cells. **a** Norway spruce seedling showing the presence and absence of epitopes in sieve cells (Sc) and (axial/ray) parenchyma cells (P/R), respectively. Note more abundant epitopes in thickened sieve cells of late phloem (marked *1–4*) than those of early phloem and the absence of epitopes in thin-walled sieve cells of later phloem (marked *6–8*). Epitopes were absent in convex cells (marked *5*) and thin-walled unspecified cells (*asterisks*). **b**, **c** Immunogold labeling of Norway spruce seedling showing overall uniform distribution of epitopes across thickened sieve cell wall (except for the innermost layer) and the absence of epitopes in middle lamellae (**b**) and axial parenchyma cell wall (**c**). **d** Scots pine seedling showing the presence and absence of epitopes in sieve- and parenchyma cells, respectively. Note similar amount of epitopes in thickened sieve cells between late (marked *1–5*) and early phloem (i.e., differ from spruce seedling). Epitopes were absent in thin-walled unspecified (*asterisks*)- and sieve cells (marked *6*) as shown in spruce (**a**). **e**, **f** Mature Norway spruce and Scots pine, respectively, showing the presence and absence of epitopes in sieve- and parenchyma cells, respectively, as shown in seedlings (**a**, **d**). Note the absence of epitopes in middle lamellae of sieve cells. *Ca* cambium. *Scale bars* 25 µm (**a**, **d**–**f**), 500 nm (**b**, **c**)

antibodies (Verhertbruggen et al. 2009). Spruce seedlings (Fig. 4a) showed much more abundant LM19 epitopes in sieve cells than the other three tree samples (Fig. 4d–f). Apart for sieve cells of late phloem (marked 1–8 in Fig. 4a), spruce seedlings revealed similar amounts of epitopes in sieve cells between radial- and tangential cell walls (Fig. 4a). In contrast, other tree samples showed no/or sparse LM19 epitopes in radial sieve cell walls across the phloem (Fig. 4d–f). Unlike sieve cells, LM19 epitopes were abundantly detected in both radial- and tangential cell walls of convex cells in spruce samples (marked 5 in Fig. 4a and asterisks in Fig. 4e). In axial parenchyma cells, LM19 epitopes were mostly absent in all tree samples. The only exception was some axial parenchyma cells that showed LM19 epitopes in the boundary between adjacent parenchyma cells, particularly between axial- and ray parenchyma cells (arrowheads in Fig. 4a, d–f). LM19 epitopes in ray parenchyma cells were only detected in tangential cell walls (arrows in Fig. 4a, d–f). No LM19 epitopes were detected in radial cell walls of ray parenchyma in any of the tree samples. Immunogold labeling confirmed that fluorescence labeling of LM19 epitopes between axial parenchyma- and sieve cells (Fig. 4a) was only produced from sieve cell cells including middle lamellae (Fig. 4c). LM19 epitopes in sieve cells of spruce seedlings were more abundant in the inner (lumen side)- than outer cell walls (Fig. 4b).

Overall distribution patterns of LM20 epitopes in spruce seedlings were opposite to those of LM19 epitopes. LM20 epitopes were more abundant in sieve cells of late phloem (marked 1–8 in Fig. 5a) compared to sieve cells of early phloem (Fig. 5a). Immunogold labeling also showed much more abundant label of LM20 epitopes in sieve cells of late phloem including middle lamellae (Fig. 5b) compared to those of early phloem (Fig. 5c) that revealed relatively sparse and high variations in the amount of epitopes between cells including absence of epitopes (not shown). The only exception was sieve cells of early phloem that showed abundant LM20 epitopes in the cell wall in contact with parenchyma cells (Fig. 5d). Unlike LM19 (Fig. 4b), LM20 epitopes in sieve- and axial parenchyma cells were mostly detected in outer cell wall regions (Fig. 5d, e). Other tree samples also showed overall similar distribution patterns of LM20 epitopes in parenchyma- and sieve cells to spruce seedling (Fig. 5f, Supplementary Fig. 3). Overall, more abundant epitopes were detected in radial- than tangential sieve cell walls in early phloem of pine seedlings and across the phloem of mature trees (Fig. 5f, Supplementary Fig. 3).

Detection of hemicellulose epitopes in sieve- and parenchyma cells

LM15 directed to the XXXG motif of xyloglucans (Marcus et al. 2008) bound to all sieve- and parenchyma cell walls. Overall, distribution patterns of LM15 epitopes were similar in the two spruce samples (i.e., seedling and mature tree) and mature pine. These tree samples showed similar amounts of LM15 epitopes between sieve- and parenchyma cell walls and more abundant epitopes in the inner- than outer sieve cell wall (Fig. 6a, d, e). In contrast, pine seedlings showed more abundant LM15 epitopes in sieve- than parenchyma cell walls (Fig. 6c). Distribution of LM15 epitopes in sieve cell walls was also more uniform and much more abundant in pine seedlings (Fig. 6c) than in the other three tree samples (Fig. 6a, d, e). Using TEM of spruce seedlings, LM15 epitopes were mostly detected in the inner layer of thickened sieve cell walls (Fig. 6b). Only exception was a few sieve cells that showed uniform distribution of epitopes across the cell wall (inset in Fig. 6b).

Distribution of heteromannans was examined using LM21 and LM22 antibodies that recognize a variety of mannan polymers with slight difference in labeling patterns (Marcus et al. 2010). Overall spruce (Fig. 7a, e) showed slightly more abundant LM21 epitopes than pine (Fig. 7d, f) in both seedling and mature trees. In spruce, sieve cells of late phloem (marked 1–4) showed more abundant LM21 epitopes than those of early phloem (Fig. 7a). No LM21 epitopes were detected in middle lamellae of sieve cells and parenchyma cell walls in all tree samples (Fig. 7). With gold labeling in spruce seedling, LM21 epitopes were evenly localized across sieve cell walls except for the innermost cell wall layer (cell lumen side) (Fig. 7b). No LM21 epitopes were detected in middle lamellae of sieve cells and axial parenchyma cell walls (Fig. 7b, c) as shown in immunofluorescence labeling. Compared to LM21 epitopes, LM22 epitopes were much less detected in all tree samples (Supplementary Fig. 4). Two seedlings showed some weak LM21 epitopes in sieve cell walls, particularly early phloem. Almost no LM22 epitopes were detected in two mature trees even though both epitopes were abundantly detected in xylem tracheids (Supplementary Fig. 4) and phloem stone cells (Fig. 9k, l). This may be related to the different binding properties between LM21 and LM22 antibodies as suggested by Marcus et al. (2010).

LM10 (Fig. 8a) and LM11(not shown) antibodies that recognize un-/and low substituted- and low-/and highly substituted xylans, respectively (McCartney et al. 2005) did not bind to any sieve- and parenchyma cells in any of the tree samples.

Detection of hemicellulose epitopes in sieve- and parenchyma cells after enzymatic removal of pectic HG

To explore pectic HG masking on recognition of hemicellulose epitopes, sections were pre-treated with sodium carbonate (pH 11.4), followed by pectate lyase (PL) prior to

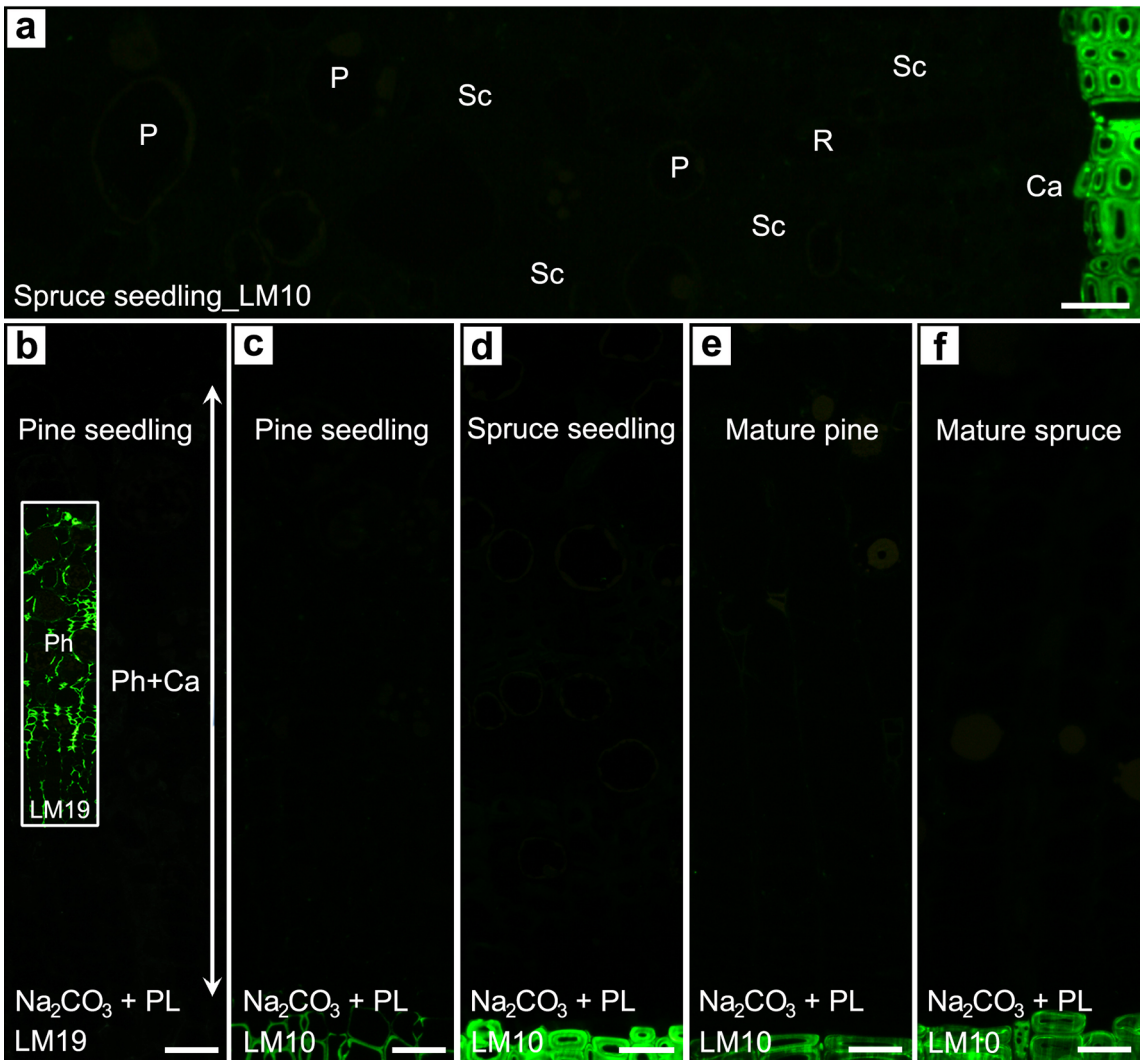

Fig. 8 Detection of heteroxylan (LM10) epitopes in phloem cells. **a** Norway spruce seedling showing the absence of LM10 epitopes in all sieve (Sc)- and (axial/ray) parenchyma cells (P/R). **b** Scots pine seedling showing the enzymatic (pectate lyase, PL) removal of LM19 homogalacturonan (HG) epitopes. The *inset* indicates LM19 epitopes without PL pre-treatment (i.e., control). **c–f** Detection of LM10 epitopes after enzymatic removal of HG (sodium carbonate + PL) showing the absence of LM10 epitopes in Scots pine (seedling/mature, **c/e**) and Norway spruce (seedling/mature, **d/f**). *Ca* cambium, *Ph* phloem. *Scale bars* 25 µm

immunolocalization. After this pre-treatment, LM19 HG epitopes (Fig. 8b) were almost non-detectable in the phloem of all tree samples compared to control (inset in Fig. 8b), which indicated optimal removal of HG from sections. Serial sections were also pre-treated only with sodium carbonate prior to immunolocalization. In all tree samples, sections pre-treated only with sodium carbonate showed slightly higher levels of LM15 (xyloglucan) and LM21 (heteromannan) epitopes compared to controls (Fig. 9, Supplementary Figs. 5, 6). However, after enzymatic removal of HG (i.e., sodium carbonate + PL), only mature spruce and pine showed notable increase in the amount of LM15 (Fig. 9b, h vs. c, i) and LM21 (Fig. 9e, k vs. f, l) epitopes compared to sections pre-treated only with sodium carbonate. The two seedling samples pre-treated with sodium carbonate and PL showed similar (LM21) or even slightly lower (LM15) amount of epitopes compared to sections pre-treated only with sodium carbonate (Supplementary Figs. 5, 6). Concerning spatial distribution patterns of LM15 and LM21 epitopes after pre-treatments, no notable differences were detected in all tree samples compared to controls. Pre-treated sections also showed more abundant LM15 epitopes in the inner- than outer sieve cell wall (Fig. 9b, c, h, i) and the absence of LM21 epitopes in parenchyma cell walls (i.e., only in sieve cells) (Fig. 9e, f, k, l) compared with controls (Fig. 9a, d, g, j). Pre-treatments did not induce any changes in detection of heteroxylan epitopes. No LM10 epitopes were detected in any sieve- or parenchyma cells in any tree samples even after pre-treatments (Fig. 8c–f) and were similar as controls (Fig. 8a).

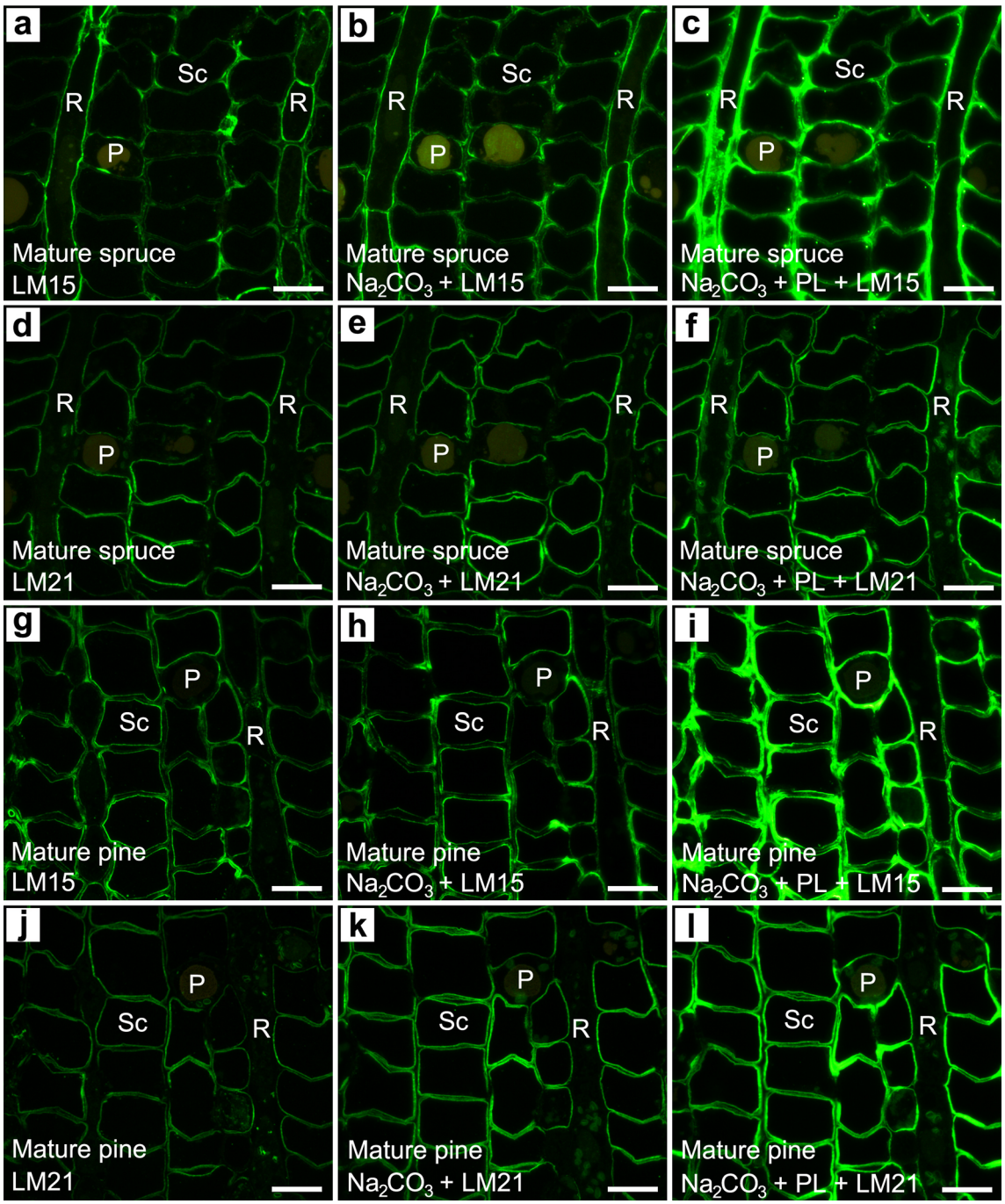

Fig. 9 Detection of xyloglucan (LM15) and heteromannan (LM21) epitopes in phloem cells of mature Norway spruce (**a**–**f**) and Scots pine (**g**–**l**) after pre-treatment with sodium carbonate (Na_2CO_3) and pectate lyase (PL). **a**–**f** and **g**–**l** are serial sections. Sections pre-treated with sodium carbonate (**b**, **e**, **h**, **k**) or sodium carbonate + PL (**c**, **f**, **i**, **l**) showing increase in the amount of LM15 (**b**, **c**, **h**, **i**) and LM21 (**e**, **f**, **k**, **l**) epitopes compared to those in controls (**a**, **d**, **g**, **j**). Note more abundant epitopes on sections pre-treated with sodium carbonate + PL (**c**, **f**, **i**, **l**) than those treated only with sodium carbonate (**b**, **e**, **h**, **k**). *P* axial parenchyma cell, *R* ray parenchyma cell, *Sc* sieve cell. *Scale bars* 25 µm

Detection of pectin and hemicellulose epitopes in stone cell walls

Stone cells in mature spruce phloem had thick secondary cell walls and frequently gathered together (Fig. 10a). Pectin epitopes were only detected in middle lamellae of stone cells (Fig. 10b–g). With localization of RG-I epitopes, LM6 epitopes were detected in middle lamellae (Fig. 10d), whereas LM5 epitopes were absent (Fig. 10c). LM19 and LM20 detecting presence of HG interacted only

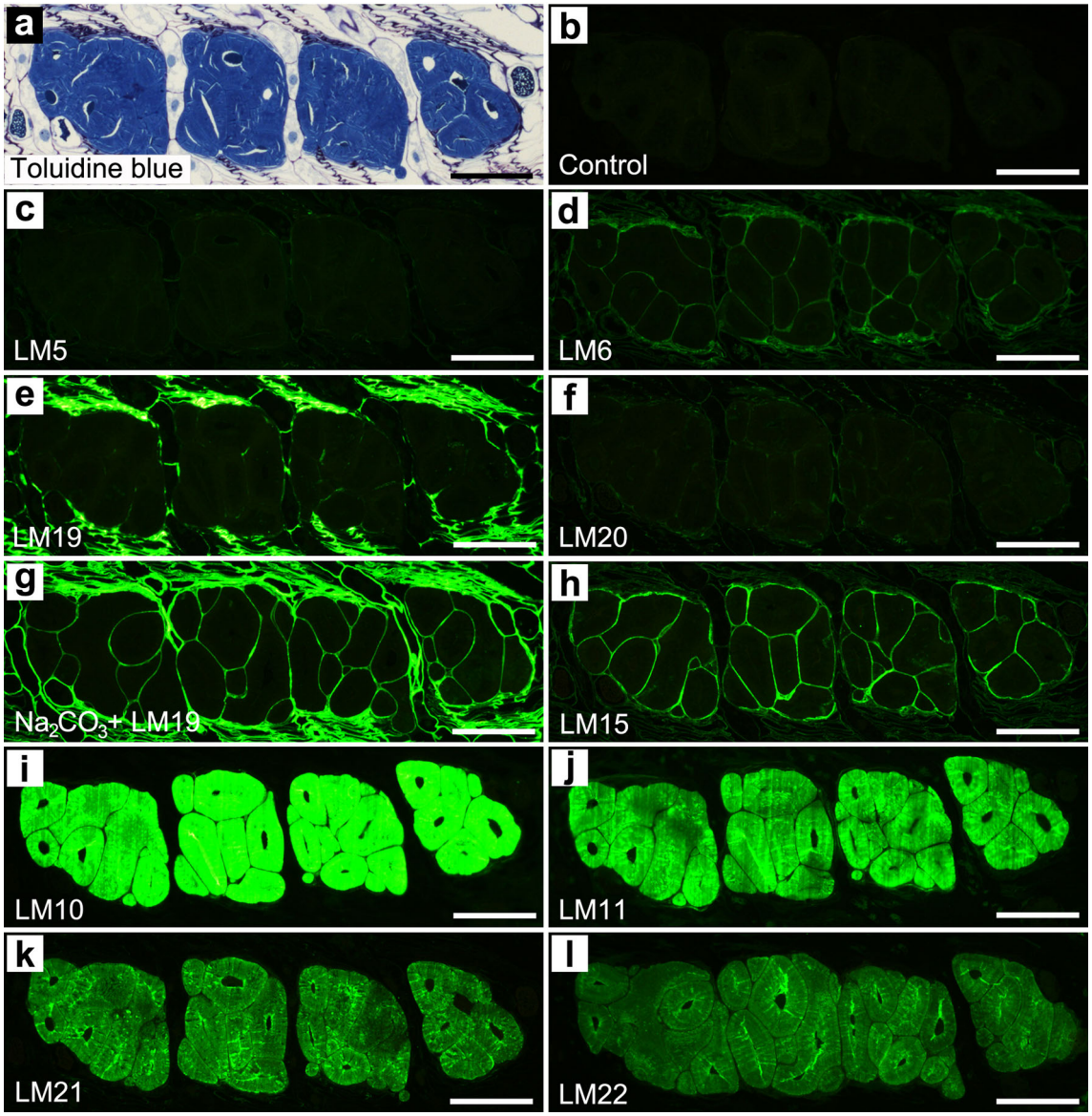

Fig. 10 Detection of pectin and hemicellulose epitopes in stone cells of Norway spruce phloem. **a–l** are serial sections. **a** Clustered stone cells stained with toluidine blue. **b** Control with primary antibody omitted. **c–g** Detection of pectin epitopes showing no, abundant and sparse LM5 galactan (**c**), LM6 arabinan (**d**) and LM19/20 homogalacturonan (**e**, **f**) epitopes in middle lamellae (ML), respectively. Note significantly increased LM19 epitopes in ML on sections pretreated with sodium carbonate (Na_2CO_3) prior to immunolabeling (**g**). **h–l** Detection of hemicellulose epitopes showing abundant LM15 xyloglucan (**h**) epitopes in ML and abundant LM10/LM11 heteroxylan (**i**, **j**) and LM21/LM22 heteromannan (**k**, **l**) epitopes in secondary cell walls. *Scale bars* 100 µm

restrictively and weakly in middle lamellae of stone cells (Fig. 10e, f). The distribution of HG in middle lamellae of stone cells was more precisely defined by pre-treatment of sections with sodium carbonate prior to immunolocalization. After this treatment, LM19 epitopes increased significantly in middle lamellae of stone cells (Fig. 10g). With hemicellulose epitopes, LM15 (xyloglucan) epitopes were only abundantly detected in middle lamellae of stone cells (Fig. 10h). In contrast, heteroxylan (LM10/LM11; Fig. 10i, j) and heteromannan (LM21/LM22; Fig. 10k, l) epitopes were abundantly detected in secondary cell walls of stone cells. These epitopes were almost undetectable in middle lamellae of stone cells (Fig. 10i–l).

Discussion

Potential effects of HG masking on detection of hemicellulose epitopes

Together with the efforts of developing new glycan-directed probes, recent studies have also examined potential

effects of the associations between cell wall components on detection of polysaccharide epitopes in plant cell walls. In particular, significant masking effects of pectic homogalacturonan (HG) on detection of hemicellulose epitopes have been reported in several annual plant cell walls (Hervé et al. 2009; Kim and Daniel 2012a, b; Marcus et al. 2008, 2010). Using the same methodology carried out in previous studies (Hervé et al. 2009; Marcus et al. 2008, 2010) we also tested HG masking effects on detection of hemicellulose epitopes in phloem cells.

The enzymatic removal of HG from sections resulted in a notable increase of LM15 xyloglucan and LM21 heteromannan epitopes in mature tree samples without notable changes in spatial distribution patterns of the epitopes (Fig. 9). However, the effect of HG removal on detection of LM15 and LM21 epitopes was not significant in the two seedling samples (Supplementary Figs. 5, 6). These results indicate that the potential effect of pectic HG masking on recognition of xyloglucan and heteromannan epitopes in phloem cells differs between mature trees and seedlings. However, at present the reason for difference in HG masking between mature trees and seedlings remains unclear. In addition to the effect of HG masking, all tree samples showed a slight increase in LM15 and LM21 epitopes by pre-treatment with only sodium carbonate, which is known to remove methyl esters from pectic HG and therefore increase PL activity in plant cell walls (Lee and Knox 2014). There are several possible explanations. First, the removal of methyl esters from HG simply increased accessibility for the LM15 and LM20 antibodies. Second, pre-treatment with sodium carbonate increased the accessibility of antibodies through changes in section surface, such as the removal of resin residuals and unknown modification in cell wall structure. It is also possible that pre-treatment with sodium carbonate removed acetyl groups from xyloglucans and heteromannans, thereby increasing the accessibility of antibodies as reported in previous studies (Handford et al. 2003; Kim et al. 2010). It is well known that polysaccharides including xyloglucans and heteromannans are normally acetylated to various degrees in plant cell walls (Scheller and Ulvskov 2010). With heteroxylans, epitopes were not detected in the phloem of all tree samples, regardless of enzymatic removal of HG and deacetylation (Fig. 8). This may indicate that the amount of heteroxylans is either very low (i.e., undetectable by antibodies) or absent in phloem sieve- and parenchyma cells.

It is important to note that apart from HG masking on detection of hemicellulose epitopes examined in this study, there are several other possibilities of masking of epitopes, such as masking of pectin and hemicellulose epitopes by other polysaccharides (Lee et al. 2013; Xue et al. 2013). There is also the potential masking effect of lignin on detection of pectin and hemicellulose epitopes in stone cells. These aspects emphasize that results of this study should be interpreted on various possibilities of masking that are not examined. Further studies using different probes combined with various pre-treatments will provide more detailed information on the in situ distribution of a single pectin and hemicellulose component. A large number of probes including antibodies and carbohydrate binding modules (CBMs) are currently available for localization of pectin and hemicellulose epitopes (e.g., Buffetto et al. 2015; Cornuault et al. 2015; Pattathil et al. 2010).

Distribution of pectin and hemicellulose epitopes in the phloem of Norway spruce and Scots pine

Unlike mature trees, the two conifer seedlings showed notable differences in distribution patterns of epitopes in sieve cells between the two different anatomical regions of phloem (i.e., early and late phloem). There are two possible explanations depending on interpretation of developmental stages of sieve cells in late phloem. First, if the sieve cells in late phloem are not fully mature even though sieve cell walls are thickened like those in early phloem, results would suggest that chemical features of sieve cells may be changed with aging. Second, in the opposite case (i.e., mature stage of development) results suggest that there are originally two types of sieve cells with different chemical features in seedlings. The following discussion focuses mainly on the chemical feature of early phloem in seedlings since developmental stages of late phloem in seedlings were unclear. Comparison with mature trees may also be more reasonable since these trees showed the end of cambial growth (i.e., mature stage of phloem).

Overall distribution patterns of pectin and hemicellulose epitopes in phloem cells of Norway spruce and Scots pine are briefly summarized in Table 1. Distribution patterns of epitopes in sieve- and parenchyma cell walls were qualitatively similar between the two tree species, regardless of tree age. RG-I, HG, xyloglucan and heteromannan (only in sieve cells) epitopes were detected in the two tree species, whereas heteroxylan epitopes were not detected. However, quantitatively the two tree species showed some notable differences (i.e., difference in intensity of fluorescence signal) in seedlings. For example, overall LM19 low methyl-esterified HG epitopes in sieve cell walls were much more abundant in Norway spruce- than Scots pine seedlings (Table 1; Fig. 4a, d), whereas LM6 arabinan and LM15 xyloglucan epitopes in sieve cell walls showed opposite patterns to LM19 epitopes (Table 1). Presumably, these results may reflect structural diversities and/or actual differences in the amount of pectins and xyloglucans in

Table 1 Distribution of pectin and hemicellulose epitopes in Norway spruce and Scots pine phloem cells as reflected by immunofluorescence labeling

Phloem cell	Wood species	RG-I		HG		XyG	Heteromannan		Heteroxylan	
		LM5	LM6	LM19	LM20	LM15	LM21	LM22	LM10	LM11
Sieve cell	Seedling									
	Spruce	−/tr	+	+++	+	++	++	tr/+	−	−
	Pine	−/tr	+++	(−/++)	(+/+++)	+++	++	tr/+	−	−
	Mature									
	Spruce	−/tr	++	(−/++)	(+/+++)	++	++	−	−	−
	Pine	−/tr	++	(−/++)	(+/+++)	++	++	−	−	−
Parenchyma cell (P/R)	Seedling									
	Spruce	tr/+	+++	(−/++)	+++	+	−	−	−	−
	Pine	tr/+	+++	(−/++)	+++	+	−	−	−	−
	Mature									
	Spruce	tr/+	+	(−/++)	++	+	−	−	−	−
	Pine	tr/+	+	(−/++)	++	+	−	−	−	−
Stone cell	Mature spruce									
	SW	−	−	−	−	−	++	++	+++	++
	ML	−	+	tr (+++)	tr (−)	+++	−	−	−	−

Data in seedlings refers to early phloem. In brief, number of '+' indicates intensity of labeling. 'tr' trace labeling, '−' no specific labeling. Parenthesis in sieve- and parenchyma cells indicates high variation in amounts of epitopes between cell wall orientations (i.e., tangential- and radial cell walls) and between cell wall regions. Parenthesis in stone cells indicates intensity of labeling after pre-treatment with sodium carbonate

P/R axial/ray parenchyma cell, *SW* secondary cell wall, *ML* middle lamella, *RG-I* rhamnogalacturonan-I, *HG* homogalacturonan, *XyG* xyloglucan

phloem cells between two tree seedlings. Compared to seedlings, the differences between two tree species were much less significant and sometimes even unclear in mature trees (Table 1). This result and together with the difference in the effect of HG masking between mature trees and seedlings as outlined above suggest that we should pay special attention to the selection of samples and generalization of chemical features of conifer phloem.

Heterogeneity in the distribution of pectin and hemicellulose epitopes between cell types and between cell wall layers

With detection of pectin epitopes, clear difference between sieve- and parenchyma cells was only detected in Norway spruce seedling with distribution of LM19/LM20 HG epitopes (Table 1; Figs. 4, 5). LM19 low methyl-esterified HG epitopes were more abundant in sieve- than parenchyma cell walls, whereas LM20 high methyl-esterified HG epitopes showed opposite labeling to LM19 in spruce seedling. These results suggest structural differences in HG between sieve- and parenchyma cells in Norway spruce seedlings. Although the other samples also showed some differences in distribution of LM19/LM20 HG epitopes between sieve- and parenchyma cells, comparison of results were difficult since there were considerable variations between cell wall orientations (i.e., tangential- and radial cell walls) and between cell wall regions in the two cell types (Table 1; Figs. 4, 5). Thus, it is evident that there are high variations in chemical structure of HG even within single sieve- and parenchyma cells depending on cell wall orientation and region.

It is of interest that LM19 low methyl-esterified HG epitopes were detected in tangential cell wall of ray parenchyma but were only detected in radial cell wall regions when in contact with axial parenchyma cells even though LM20 high methyl-esterified HG epitopes were detected in all ray parenchyma cell wall regions (Figs. 4, 5). These results indicate that the degree of esterification in HG is much lower in tangential- than radial cell walls (except for radial cell walls in ray-axial parenchyma contact) even within the same ray parenchyma cell. This structural difference of HG in tangential- compared with radial cell walls is likely related to the radial transport between xylem and phloem since the tangential cell wall in ray parenchyma cell is a main gate for xylem–phloem interactions.

With hemicelluloses, there was a clear difference in distribution of LM21 heteromannan epitopes between

sieve- and parenchyma cells. Heteromannan epitopes were only detected in sieve cell walls and not in parenchyma cell walls (Table 1). In general, plant mannans are divided into linear mannan, glucomannan, galactomannan, and galactoglucomannan subfamilies (Moreira and Filho 2008). Galactoglucomannans are typical mananns present in softwood xylem and occupy approximately 20–25% of cell wall components (Fengel and Wegener 1989). It is generally considered that heteromannans play a role as structural polysaccharides in wood cell walls and contribute to the physical properties of cell walls. This suggests that heteromannans, probably galactoglucomannans, in sieve cell walls may ensure proper physical properties of the cell wall, such as strength, flexibility and firmness for long-distance transportation of assimilates, which is the main role of sieve cells in conifer phloem. Parenchyma cell walls may be separated from physical properties than sieve cell walls since parenchyma cells in phloem function mainly for storage.

Immunogold labeling with Norway spruce seedlings further indicates that there are considerable differences in the microdistribution of epitopes even within the single sieve cell wall. Inner sieve cell walls (cell lumen side) showed more abundant LM6 arabinan (Fig. 3b), LM19 low methyl-esterified HG (Fig. 4b) and LM15 xyloglucan (Fig. 6b) epitopes than the outer cell walls. In contrast, the outer sieve cell walls revealed more abundant LM20 high methyl-esterified HG epitopes than the inner cell walls (Fig. 5b, c). These results indicate heterogeneity of chemistry within individual sieve cell walls. However, at present it is unclear how this chemical heterogeneity influences physical and biological function of the sieve cells.

Distribution of pectins and hemicelluloses in stone cell walls

Stone cells are found in many of the Pinaceae and vary in the amount and type between tree species (Franceschi et al. 2005). A stone cell has generally thickened and lignified secondary cell walls like the stone cells in Norway spruce in this study (Franceschi et al. 2005; Whitehill et al. 2015). Results demonstrate that heteroxylans and heteromannans are major non-cellulosic polysaccharides in secondary cell walls of phloem stone cells in Norway spruce (Table 1). A similar result was also reported by Whitehill et al. (2015) who found abundant heteroxylan (using LM10 antibody) and heteromannan (using BGM C6 antibody) epitopes in secondary cell walls of cortex stone cells in Sitka spruce. In contrast to secondary cell walls, results show that pectins (RG-I, HG) and xyloglucans are major non-cellulosic polysaccharides in middle lamellae of phloem stone cells (Table 1). These labeling patterns in secondary cell walls and middle lamellae are qualitatively similar to those of xylem tracheids. However, Whitehill et al. (2015) reported that heteroxylans in cortex stone cells of Sitka spruce is quantitatively almost three times higher than heteromannans, i.e., opposite to xylem tracheids, in which heteromannan content is much higher than heteroxylans. Compared to thickened sieve cell walls that were also considered as secondary cell walls (Abbe and Crafts 1939; Evert 1977), secondary cell walls of stone cells showed difference in the distribution of heteroxylan epitopes (i.e., absence in sieve cells vs. presence in stone cells). These results indicate that the occurrence of heteroxylans in secondary cell walls is likely related to lignification since secondary cell walls of stone cells (also xylem tracheids) are lignified (Supplementary Fig. 2), whereas secondary cell walls of sieve cells are non-lignified, but further studies are required. Donaldson and Knox (2012) suggested that lignification of wood cell walls may be mediated by changes in the amount and distribution of heteromannans and heteroxylans.

Conclusions

Immunolocalization of pectin and hemicellulose epitopes in the phloem of two conifer species indicates the presence of RG-I, HG, xyloglucans and heteromannans in thickened sieve cell walls and the presence of RG-I, HG and xyloglucans in parenchyma cell walls. Results also show that heteromannans/heteroxylans and RG-I/HG/xyloglucans are major non-cellulosic polysaccharides in secondary cell walls and middle lamellae of phloem stone cells, respectively. Observations also demonstrate that there is wide variation in the chemical structure and/or the amount of pectins and hemicelluloses in phloem cells between two conifer species and this variation is more significant in seedlings than mature trees. Together, this study extends our understanding of phloem chemistry from gross chemical analysis to the individual cell wall level. These findings can improve our understanding of physiochemical functions of conifer phloem and provide a basis for decomposition of softwood phloem.

Author contribution statement JSK and GD conceived and designed the study. JSK performed the experiments. JSK and GD wrote the manuscript.

Acknowledgements The authors gratefully acknowledge funding provided by Formas projects 2008-1399, 2009-582, 2011-416 and 2015-469.

Compliance with ethical standards

Conflict of interest The authors declare that they have no conflict of interest.

References

Abbe LB, Crafts AS (1939) Phloem of white pine and other coniferous species. Bot Gaz 100:695–722

Buffetto F, Cornuault V, Rydahl MG, Ropartz D, Alvarado C, Echasserieau V, Gall SL, Bouchet B, Tranquet O, Verhertbruggen Y, Willats WGT, Knox JP, Ralet M-C, Guillon F (2015) The deconstruction of pectic rhamnogalacturonan I unmasks the occurrence of a novel arabinogalactan oligosaccharide epitope. Plant Cell Physiol 56:2181–2196. doi:10.1093/pcp/pcv128

Cornuault V, Buffetto F, Rydahl MG, Marcus SE, Torode TA, Xue J, Crépeau M-J, Faria-Blanc N, Willats WGT, Dupree P, Ralet M-C, Knox JP (2015) Monoclonal antibodies indicate low-abundance links between heteroxylan and other glycans of plant cell walls. Planta 242:1321–1334. doi:10.1007/s00425-015-2375-4

Donaldson LA, Knox JP (2012) Localization of cell wall polysaccharides in normal and compression wood of radiata pine: relationships with lignification and microfibril orientation. Plant Physiol 158:642–653. doi:10.1104/pp.111.184036

Evert RF (1977) Phloem structure and histochemistry. Annu Rev Plant Physiol 28:199–222. doi:10.1146/annurev.pp.28.060177.001215

Fengel D, Wegener G (1989) Wood: chemistry, ultrastructure, reactions. de Gruyter, Berlin

Franceschi VR, Krokene P, Christiansen E, Krekling T (2005) Anatomical and chemical defenses of conifer bark against bark beetles and other pests. New Phytol 167:353–376. doi:10.1111/j.1469-8137.2005.01436.x

Handford MG, Baldwin TC, Goubet F, Prime TA, Miles J, Yu X, Dupree P (2003) Localisation and characterization of cell wall mannan polysaccharides in *Arabidopsis thaliana*. Planta 218:27–36. doi:10.1155/2014/792420

Harun J, Labosky P (1985) Chemical constituents of five northeastern barks. Wood Fiber Sci 17:274–280

Hervé C, Rogowski A, Gilbert HJ, Knox JP (2009) Enzymatic treatments reveal differential capacities for xylan recognition and degradation in primary and secondary plant cell walls. Plant J 58:413–422. doi:10.1111/j.1365-313X.2009.03785.x

Jones L, Seymour GB, Knox JP (1997) Localization of pectic galactan in tomato cell walls using a monoclonal antibody specific to (1 → 4)-*β*-D-galactan. Plant Physiol 113:1405–1412. doi:10.1104/pp.113.4.1405

Jyske T, Hölttä T (2015) Comparison of phloem and xylem hydraulic architecture in *Picea abies* stems. New Phytol 205:102–115. doi:10.1111/nph.12973

Jyske TM, Suuronen JP, Pranovich AV, Laakso T, Watanabe U, Kuroda K, Abe H (2015) Seasonal variation in formation, structure, and chemical properties of phloem in Picea abies as studied by novel microtechniques. Planta 242:613–629. doi:10.1007/s00425-015-2347-8

Kemppainen K, Inkinen J, Uusitalo J, Nakari-Setälä T, Siika-aho M (2012) Hot water extraction and steam explosion as pretreatments for entanol production from spruce bark. Bioresour Technol 117:131–139. doi:10.1016/j.biortech.2012.04.080

Kim JS, Daniel G (2012a) Immunolocalization of hemicelluloses in *Arabidopsis thaliana* stem. Part I: temporal and spatial distribution of xylans. Planta 236:1275–1288. doi:10.1007/s00425-012-1686-y

Kim JS, Daniel G (2012b) Immunolocalization of hemicelluloses in *Arabidopsis thaliana* stem. Part II: mannan deposition is regulated by phase of development and its patterns of temporal and spatial distribution differ between cell types. Planta 236:1367–1379. doi:10.1007/s00425-012-1687-x

Kim JS, Daniel G (2014) Immunocytochemical studies of axial resin canals. II. Localization of non-cellulosic polysaccharides in epithelium and subsidiary cells of Scots pine. IAWA J 35:253–269. doi:10.1163/22941932-00000064

Kim JS, Awano T, Yoshinaga A, Takabe K (2010) Temporal and spatial immunolocalization of glucomannans in differentiating earlywood tracheid cell walls of *Cryptomeria japonica*. Planta 232:545–554. doi:10.1007/s00425-010-1189-7

Knox JP (2008) Revealing the structural and functional diversity of plant cell walls. Curr Opin Plant Biol 11:308–313. doi:10.1016/j.pbi.2008.03.001

Kofujita H, Ettyu K, Ota M (1999) Characterization of the major components in bark from five Japanese tree species for chemical utilization. Wood Sci Technol 33:223–228. doi:10.1007/s002260050111

Le Normand M, Moriana R, Ek M (2014) Isolation and characterization of cellulose nanocrystals from spruce bark in a biorefinery perspective. Carbohydr Polym 111:979–987. doi:10.1016/j.carbpol.2014.04.092

Lee KJ, Knox JP (2014) Resin embedding, sectioning, and immunocytochemical analysis of plant cell walls in hard tissues. Methods Mol Biol 1080:41–52. doi:10.1007/978-1-62703-643-6_3

Lee KJD, Cornuault V, Manfield IW, Ralet M-C, Knox JP (2013) Multi-scale spatial heterogeneity of pectic rhamnogalacturonan I (RG-I) structural features in tobacco seed endosperm cell walls. Plant J 75:1018–1027. doi:10.1111/tpj.12263

Lee KJD, Sakata Y, Mau S-L, Pettolino F, Bacic A, Quatrano RS, Knight CD, Knox JP (2005) Arabinogalactan proteins are required for apical cell extension in the Moss *Physcomitrella patens*. Plant Cell 17:3051–3065. doi:10.1105/tpc.105.034413

Li S-H, Schneider B, Gershenzon J (2007) Microchemical analysis of laser-microdissected stone cells of Norway spruce by cryogenic nuclear magnetic resonance spectroscopy. Planta 225:771–779. doi:10.1007/s00425-006-0376-z

Marcus SE, Verhertbruggen Y, Hervè C, Ordaz-Ortiz J, Farkas V, Pedersen HL, Willats WGT, Knox JP (2008) Pectic homogalactronan masks abundant sets of xyloglucan epitopes in plant cell walls. BMC Plant Biol 8:60. doi:10.1186/1471-2229-8-60

Marcus S, Blake AW, Benians TAS, Lee KJD, Poyser C, Donaldson L, Leroux O, Rogowski A, Petersen HL, Boraston A, Gilbert HJ, Willats WGT, Knox JP (2010) Restricted access of proteins to mannan polysaccharides in intact plant cell walls. Plant J 64:191–203. doi:10.1111/j.1365-313X.2010.04319.x

McCartney L, Marcus SE, Knox JP (2005) Monoclonal antibodies to plant cell wall xylans and arabinoxylans. J Histochem Cytochem 53:543–546. doi:10.1369/jhc.4B6578.2005

Moreira LRS, Filho EXF (2008) An overview of mannan structure and mannan-degrading enzyme systems. Appl Microbiol Biotechnol 79:165–178. doi:10.1007/s00253-008-1423-4

Nurmi J (1997) Heating values of mature trees. Acta For Fenn 256:28p

Pattathil S, Avci U, Baldwin D, Swennes AG, McGill JA, Popper Z, Bootten T, Albert A, Davis RH, Chennareddy C, Dong R, O'Shea B, Rossi R, Leoff C, Freshour G, Narra R, O'Neil M, York WS, Hahn MG (2010) A comprehensive toolkit of plant cell wall glycan-directed monoclonal antibodies. Plant Physiol 153:514–525. doi:10.1104/pp.109.151985

Rhén C (2004) Chemical composition and gross calorific value of the above-ground biomass components of young *Picea abies*. Scand J For Res 19:72–81. doi:10.1080/02827580310019185

Scheller HV, Ulvskov P (2010) Hemicelluloses. Annu Rev Plant Biol 61:10.1–10.27. doi:10.1146/annurev-arplant-042809-112315

Umemura A, Enomoto R, Kounosu T, Orihashi K, Kato Y, Kojima Y (2014) Pyrolysis of barks from three Japanese softwoods. J Jpn Inst Energy 93:953–957. doi:10.3775/jie.93.953

Verhertbruggen Y, Marcus SE, Haeger A, Ordaz-Ortiz JJ, Knox JP (2009) An extended set of monoclonal antibodies to pectic homogalacturonan. Carbohydr Res 344:1858–1862. doi:10.1016/j.carres.2008.11.010

Whitehill JG, Henderson H, Schuetz M, Skyba O, Yuen MMS, King J, Samuels AL, Mansfield SD, Bohlmann J (2015) Histology and cell wall biochemistry of stone cells in the physical defense of conifers against insects. Plant Cell Environ 39:1646–1661. doi:10.1111/pce.12654

Willats WGT, Marcus SE, Knox JP (1998) Generation of monoclonal antibody specific to (1 → 5)-α-L-arabinan. Carbohydr Res 308:149–152

Xue J, Bosch M, Knox JP (2013) Heterogeneity and glycan masking of cell wall microstructures in the stems of *Miscanthus* × *giganteus*, and its parents *M. sinensis* and *M. sacchariflorus*. PLoS One 8:e82114. doi:10.1371/journal.pone.0082114